

# Responsible Disclosure of Generative Models Using Scalable Fingerprinting

Ning Yu<sup>1,2\*</sup> Vladislav Skripniuk<sup>3\*</sup> Dingfan Chen<sup>3</sup> Larry Davis<sup>1</sup> Mario Fritz<sup>3</sup>

<sup>1</sup>University of Maryland, College Park, United States

<sup>2</sup>Max Planck Institute for Informatics, Saarbrücken, Germany

<sup>3</sup>CISPA Helmholtz Center for Information Security, Saarbrücken, Germany

{ningyu, vladislav}@mpi-inf.mpg.de

{dingfan.chen, fritz}@cispa.saarland

lsd@cs.umd.edu

## Abstract

Over the past five years, deep generative models have achieved a qualitative new level of performance. Generated data has become difficult, if not impossible, to be distinguished from real data. While there are plenty of use cases that benefit from this technology, there are also strong concerns on how this new technology can be misused to spoof sensors, generate deep fakes, and enable misinformation at scale. Unfortunately, current deep fake detection methods are not sustainable, as the gap between real and fake continues to close. In contrast, our work enables a responsible disclosure of such state-of-the-art generative models, that allows researchers and companies to fingerprint their models, so that the generated samples containing a fingerprint can be accurately detected and attributed to a source. Our technique achieves this by an efficient and scalable ad-hoc generation of a large population of models with distinct fingerprints. Our recommended operation point uses a 128-bit fingerprint which in principle results in more than  $10^{36}$  identifiable models. Experimental results show that our method fulfills key properties of a fingerprinting mechanism and achieves effectiveness in deep fake detection and attribution.

## 1. Introduction

Over the recent five years, deep generative models have demonstrated stunning performance in generating photo-realistic images [30, 16, 33, 35], and have delivered extensive applications ranging from low-level image postprocessing [34, 49, 31, 32, 51, 42, 61] to high-level semantic-conditioned image generation [24, 53, 44, 37, 7, 45] and attribute editing [9, 10, 48, 1]. These successes are considerably boosted by the revolutionary technique of generative

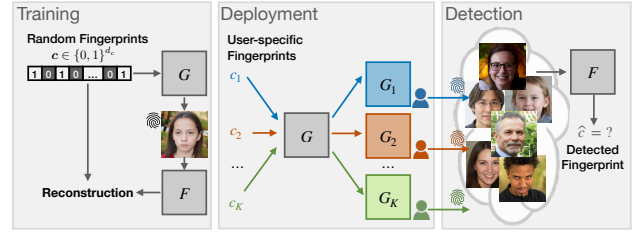


Figure 1. The diagram of our fingerprinting mechanism for generative models. We can ad-hoc generate a large number of fingerprinted generators with responsible disclosure.

adversarial networks (GANs) [16, 46, 18, 41, 3, 26, 27, 28], and are closing the gap of appearances between real images and fake ones.

Despite plenty of use cases of generative models, a flood of strong concerns arise [19, 8, 5]: how can these models be misused to spoof sensors, generate deep fakes, and enable misinformation at scale? Not only human beings have difficulties in distinguishing deep fakes, unfortunately, dedicated research efforts on deep fake detection [13, 62, 14, 60] and attribution [40, 57, 52] are unable to sustain longer against the evolution of generative models. For example, researchers delve into details on how deep fake detection works, and learn to improve generation that better fits the detection criteria [60, 12]. In principle, any successful detector can play an auxiliary role in augmenting the discriminator in the next iteration of GAN techniques, and consequently results in an even stronger generator.

The dark side of deep generative models makes its industrialization process not as straightforward as those of other artificial intelligence techniques. For example, when commercializing the GPT-2 [47] and GPT-3 [4] models, OpenAI hesitates to open-source the models but rather only release the black-box APIs<sup>1</sup>. They involve expensive human labor

\*Equal contribution.

<sup>1</sup><https://openai.com/blog/openai-api/>

in the loop to monitor and prevent the malicious use of the APIs. Yet still, it is a challenging and industry-wide task on how to trace the responsibility of the downstream use cases in an open end.

To pioneer in this task, we propose a fingerprinting mechanism to enable a responsible disclosure of deep generative models, that allows researchers and companies to fingerprint their models, so that the generated samples containing a fingerprint can be accurately detected and attributed to a source. This is achieved by an efficient and scalable ad-hoc generation of a large population of models with distinct fingerprints. See Figure 1 Middle.

Similar in the spirit of the dynamic filter networks [25] and style-based generator architectures [27, 28] where their network filters are not freely learned but conditioned on an input, we regulate to parameterize a unique fingerprint into the filters of each generator instance. The core gist is to incorporate a fingerprint auto-encoder into a GAN framework while preserving the original generation performance. See Figure 1 Left. In particular, given a GAN backbone with a generator and a discriminator, we use the fingerprint embedding from the encoder to modulate each convolutional filter of the generator (Figure 2(b)), and try to decode this fingerprint from the generated images. We jointly train the fingerprint auto-encoder and GAN with our fingerprint related losses and the original adversarial loss. See Figure 2(a) for the diagram, and 3.2 for details.

After training, the model owner is capable of fingerprinting and releasing different generator instances to different users, which are equipped with the same generation performance but with different fingerprints. As a result, when misuse of a model happens, the model owner can use the decoder to detect the fingerprint from the generated images, and then trace the responsibility of the user. See Figure 1 Right. Based on this form of responsible disclosure, model owners, like OpenAI, have a way to mitigate adverse side effects on society when releasing their powerful models, while at the same time should have an automatic way to attribute misuse.

There are several key properties of our mechanism. The **efficiency** to instantiate a generator is inherently satisfied because, after training, the fingerprint encoding and filter modulation run with little overhead. We evaluate the **effectiveness** of our fingerprinting and obtain almost perfect detection accuracy. We also justify the **fidelity** with a negligible side effect on the original generation quality. See Section 4.2. Our recommended operation point uses a 128-bit fingerprint (Section 4.3) which in principle results in more than  $10^{36}$  identifiable generator instances. The **scalability** benefits from the fact that fingerprints are randomly sampled on the fly during training so that fingerprint detection generalizes well for the entire fingerprint space. See Section 4.4 for validation. In addition, we validate in Sec-

tion 4.5 the **robustness** and **immunizability** of our fingerprinting against perturbation on generated images.

To target the initial motivation, we test our mechanism, as an active method, in the deep fake detection and attribution tasks. We show in Section 4.6 saturated performance and advantages over one of the state-of-the-art discriminative methods [57] especially in the open world. This is because, conditioned on user-specific fingerprint inputs, the presence of such fingerprints in generated images guarantees the margin between real and fake, and facilitates the attribution and responsibility tracing of deep fakes to their sources.

Our **contributions** are in four thrusts:

- (1) We introduce the concept of fingerprinting for generative models that enables a responsible disclosure of state-of-the-art GAN models.
- (2) We present a novel mechanism for efficient and scalable fingerprinting GAN models, i.e., only one generic GAN model is trained while more than  $10^{36}$  identifiable instances (each with unique fingerprint) can be obtained with little overhead during deployment.
- (3) We also justify several key properties of our fingerprinting, including effectiveness, fidelity, large capacity, scalability, robustness, and immunizability.
- (4) Finally, for the deep fake detection and attribution tasks, we validate its saturated performance and advantages over previous learning-based discriminative methods. It makes our responsible disclosure independent of the evolution of GAN techniques and orthogonal to the other detection baselines.

## 2. Related work

**Generative adversarial networks (GANs).** GANs [16] were invented to model real data distribution via solving a real/fake binary classification problem, and demonstrated stunning realism. This has triggered rapid progresses towards generating photorealistic images in high resolution [46, 18, 41, 3, 26, 27, 28]. Many successful generative applications are established on them, including but not limited to image postprocessing [34, 49, 31, 32, 51, 42, 61], image translation [24, 64, 65, 36, 23, 53, 44, 11, 43], and image manipulation [9, 10, 48, 1]. They deliver generative modeling techniques to ordinary people and make deep fakes popular on social media, which urges mitigation against deep fake misuse. As a response, our fingerprinting mechanism enables responsible disclosure of generative models, and is agnostic to the evolution and category of them. We demonstrate that our method can effectively fingerprint the state-of-the-art GAN models [28] without affecting generation quality.

**Deep fake detection and attribution.** These tasks come along with the increasing concerns on deep fake misuse [19, 8, 5]. Deep fake detection is a binary classification

problem to distinguish fake samples from real ones, while attribution further traces their sources. The findings of visually imperceptible but machine-distinguishable patterns in GAN-generated images make these tasks viable by noise pattern matching [40], deep classifiers [2, 21, 57], or deep Recurrent Neural Networks [17]. [52] follows up with a generalization of classification across different GAN techniques. [62, 13, 12, 39, 39] observe that mismatches between real and fake in frequency domain or in texture representation can facilitate deep fake detection.

However, none of these methods can sustain a long time against the adversarial iterations of GAN techniques. For example, [12] improves generation realism by closing the gap in generated high-frequency components. To handle this situation, artificial fingerprinting is proposed in [59] to be independent of GAN evolution. Yet [59] cannot scale up to a large number of fingerprints because they have to pre-process training data for each fingerprint and re-train a generator with each fingerprint. Our method is similar in spirit to [59], but possesses fundamental advantages: after training one generic fingerprinting model, we can instantiate a large number of generators ad-hoc with different fingerprints.

**Conditioned parameters in networks.** We achieve generator fingerprinting by modulating convolutional filters with fingerprint embeddings. There exist a variety of works about conditioning network parameters on the input, some using adaptive normalization [22, 44, 23, 36, 27], some using dynamic filters [25, 37, 28], and others using self/reference attention [6, 54, 15, 55, 63]. However, none of them pays attention to mitigate deep fake misuse. We pioneer in this novel direction.

### 3. GAN fingerprinting networks

We present responsible disclosure of generative models as a novel solution to mitigate deep fake misuse, which is agnostic to GAN techniques and sustainable along with their evolution. In Section 3.1 we depict how our fingerprinting mechanism enables responsible disclosure. We introduce in details our loss design in Section 3.2 and modulation design in Section 3.2.

#### 3.1. Problem statement

Generative models can be misused to spoof sensors, generate deep fakes, and enable misinformation at scale [19, 8, 5]. Researchers and companies like OpenAI lean conservative to the side effects of their powerful generative models on society. As a result, they have to provide only APIs rather than source code of their models, and limit the access to them by approving users and applications only after rigorous reviews. This notably slows down the industrialization process for the deployment of generative models.

One promising solution to mitigate model owners' concerns and enhance their regulation is to enable responsible disclosure of their models and tracing the users who misuse their models. We achieve this by equipping owners with a model fingerprinting auto-encoder, such that they can use the encoder to efficiently instantiate a large population of models with the same generation performance but with distinct fingerprints. As a result, model owner can release different model instances to different users. When misuse of a model happens, model owner can use the decoder to detect the fingerprint from the generated images, and then trace the responsibility of the user. Based on this form of responsible disclosure, model owners, like OpenAI, should feel safer and be stressed less by the society when releasing their powerful models, while at the same time should have an automatic way to attribute misuse cases.

#### 3.2. Loss design

We list symbol notations at the beginning. We use latent code  $z \sim \mathcal{N}(\mathbf{0}, \mathbf{I}^{d_z})$  to control generated content. We represent fingerprint  $c \sim \text{Ber}(0.5)^{d_c}$  as a sequence of bits. It follows Bernoulli distribution with probability 0.5. We non-trivially choose the fingerprint length  $d_c$  in Section 4.3. We denote encoder  $E$  mapping  $c$  to its embedding, generator  $G$  mapping  $(z, E(c))$  to the image domain, discriminator  $D$  mapping an image  $x \sim p_{\text{data}}$  to the real/fake classification probability, and decoder  $F$  mapping an image to the decoded latent code and fingerprint  $(\hat{z}, \hat{c})$ . In the following formulations, we denote  $G(z, E(c))$  as  $G(z, c)$  for brevity.

We consider three goals in our training. First, we preserve the original functionality of GANs to generate realistic images, as close to real distribution as possible. We use the unsaturated logistic loss as in [16, 27, 28] for real/fake binary classification:

$$\mathcal{L}_{adv} = \mathbb{E}_{x \sim p_{\text{data}}} \log D(x) + \mathbb{E}_{\substack{z \sim \mathcal{N}(\mathbf{0}, \mathbf{I}^{d_z}) \\ c \sim \text{Ber}(0.5)^{d_c}}} \log(1 - D(G(z, c))) \quad (1)$$

In addition, similar to [50], we reconstruct the latent code through the decoder  $F$  to augment generation diversity and mitigate the mode collapse issue of GANs [50, 35, 58].

$$\mathcal{L}_z = \mathbb{E}_{\substack{z \sim \mathcal{N}(\mathbf{0}, \mathbf{I}^{d_z}) \\ c \sim \text{Ber}(0.5)^{d_c}}} \sum_{k=1}^{d_z} \left( z_k - F(G(z, c))_k \right)^2 \quad (2)$$

where we use the first  $d_z$  output elements of  $F$  that correspond to the decoded latent code.

The second goal is to reconstruct the fingerprint so as to

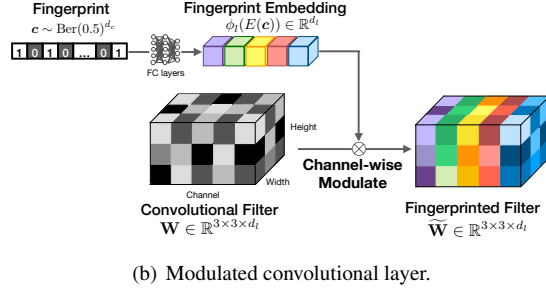
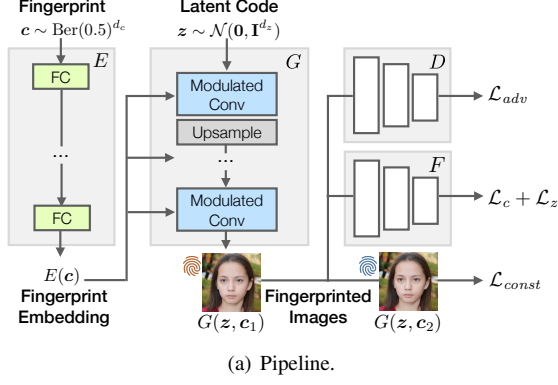


Figure 2. The diagram of our fingerprinting pipeline and the zoom-in of the modulated convolutional layer.

enable our core functionality of fingerprint detection.

$$\mathcal{L}_c = \mathbb{E}_{\substack{z \sim \mathcal{N}(\mathbf{0}, \mathbf{I}^{d_z}) \\ c \sim \text{Ber}(0.5)^{d_c}}} \sum_{k=1}^{d_c} c_k \log \sigma(F(G(z, c))_{d_z+k}) + (1 - c_k) \log(1 - \sigma(F(G(z, c))_{d_z+k})) \quad (3)$$

where we use the last  $d_c$  output elements of  $F$  that correspond to the decoded fingerprint.  $\sigma(\cdot)$  denotes the sigmoid function and the reconstruction is a combination of binary classification for each bit.

It is worth noting that we use one decoder to decode both the latent code and fingerprint, which benefits for cooperating between them so as to explicitly disentangle their representations as discussed below.

The third goal is to disentangle the representation between latent code and fingerprint. Desirably, latent code should have an exclusive control to the generated content. This sticks to the original generation functionality. Therefore, two images with different fingerprints but with identical latent code should have consistent appearance. We formulate the consistency loss as:

$$\mathcal{L}_{const} = \mathbb{E}_{\substack{z \sim \mathcal{N}(\mathbf{0}, \mathbf{I}^{d_z}) \\ c_1, c_2 \sim \text{Ber}(0.5)^{d_c}}} \|G(z, c_1) - G(z, c_2)\|_2^2 \quad (4)$$

The disentangled effect is demonstrated in Figure 3.

Our final training objective is as follows. We optimize it under the adversarial training framework w.r.t.  $E$ ,  $G$ ,  $F$ , and  $D$ .

$$\min_{E, F, G} \max_D \lambda_1 \mathcal{L}_{adv} + \lambda_2 \mathcal{L}_z + \lambda_3 \mathcal{L}_c + \lambda_4 \mathcal{L}_{const} \quad (5)$$

where  $\lambda_1 = 1.0$ ,  $\lambda_2 = 1.0$ ,  $\lambda_3 = 2.0$ , and  $\lambda_4 = 2.0$  are hyper-parameters to balance the magnitude of each loss term. See Figure 2(a) for the diagram.

### 3.3. Fingerprint modulation

At the architectural level, it is non-trivial how to embed  $E(c)$  into  $G$ . The gist is to embed fingerprint into the generator parameters rather than generator input, so that (1) our mechanism is agnostic to the architecture of a GAN model, and (2) after training a generic model we can instantiate a large population of generators ad-hoc with different fingerprints. The second point is a critical advantage to make our fingerprinting efficient and scalable, as validated in Section 4.4. We then deploy only the fingerprinted generator instances, not including the encoder.

We achieve this by modulating convolutional filters in the generator backbone with our fingerprint embedding, similar in spirit of [28]. Given a convolutional kernel  $\mathbf{W} \in \mathbb{R}^{3 \times 3 \times d_l}$  at layer  $l$ , we first project the fingerprint embedding  $E(c)$  through an affine transformation  $\phi_l$  such that  $\phi_l(E(c)) \in \mathbb{R}^{d_l}$ . The transformation is implemented as a fully-connect neural layer with learnable parameters. We then scale each channel of  $\mathbf{W}$  with the corresponding value in  $\phi_l$ . In specific,

$$\tilde{\mathbf{W}}_{i,j,k} = \phi_l(E(c))_k \cdot \mathbf{W}_{i,j,k}, \quad \forall i, j, k \quad (6)$$

See Figure 2(b) for a diagram illustration. We compare to the other fingerprint embedding architectures in Section 4.2 and validate the advantages of this one. We conduct modulation for all the convolutional filters at layer  $l$  with the same fingerprint embedding. And we investigate in Section 4.7 at which layer to modulate we can achieve the optimal performance. A desirable trade-off is to modulate all convolutional layers.

Note that, during training, latent code  $z$  and fingerprint  $c$  are jointly sampled. Yet for deployment the model owner first samples a fingerprint  $c_0$ , then modulates the generator  $G$  with  $c_0$ , and then deploys only the modulated (fingerprinted) generator  $G(\cdot, c_0)$  to a user. For that user there allows only one input, i.e. the latent code, to the modulated generator. The encoder  $E$ , decoder  $F$ , and discriminator  $D$  are all unavailable to the user. Once a misuse happens, the model owner uses the decoder to decode the fingerprint and attribute it to the user, so as to achieve responsible disclosure.



## 4. Experiments

We describe the experiment settings in Section 4.1. We validate several key properties of a fingerprint mechanism from Section 4.2 to 4.5. We then apply our mechanism to deep fake detection and attribution in Section 4.6. We conduct an ablation study on filter modulation in Section 4.7.

### 4.1. Setup

**Datasets.** We conduct experiments on CelebA human face dataset [38] and LSUN bedroom scene dataset [56], which are common datasets for image generation experiments. We train/evaluate on 30k/30k CelebA, and 30k/30k LSUN at the size of  $128 \times 128 \times 3$ .

**GAN backbone.** Our fingerprinting mechanism is agnostic to GAN configurations. We build upon the most recent state-of-the-art StyleGAN2 [28] config E. One modification happens to how we input the latent code. Instead of encoding them through filter modulation, we find that directly feeding it through the input of the generator achieves better results. See Section 4.2. Our model is trained from scratch with the original training protocol provided by [28].

### 4.2. Effectiveness and fidelity

**Evaluation.** The effectiveness indicates that the input fingerprints consistently present in the generated images and can be accurately detected by the decoder. This is measured by fingerprint detection bitwise accuracy over 30k random samples (with random latent codes and random fingerprint codes). A larger value is more desirable. We use 128 bits to represent a fingerprint. This is a non-trivial setting as analyzed in Section 4.3. We also provide the  $p$ -value to accept a null hypothesis that the detected fingerprint is composed of random guesses rather than a reconstruction of the input fingerprint. It is calculated from the binomial probability distribution with  $d_c$  trials, where  $d_c$  is the number of bits. Therefore, a smaller  $p$ -value is more desirable, and should be smaller than 0.05 to reject the null hypothesis. We regard  $1 - p$  as the confidence of our detection.

The fidelity reflects how imperceptible the original generation performance is affected by fingerprinting. It also helps avoid one’s suspect of the presence of fingerprints which may attract adversarial fingerprint removal. Fréchet Inception Distance (FID) [20] is the standard measure for generation quality. We report FID between 30k generated images and 30k real testing images. A smaller value indicates the generated images are more realistic in general.

**Baseline methods.** We compare to five baseline methods. The first baseline is the StyleGAN2 [28] backbone with the original architecture: the latent code is encoded through filter modulation. It provides the upper bound of fidelity while has no fingerprinting functionality.

The second baseline is [59] which is the other active fingerprinting method for GANs. However, regardless of its

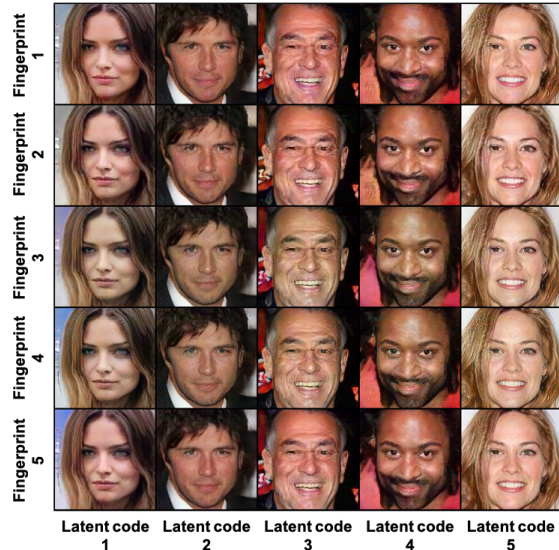


Figure 3. Generated samples from five of our generator instances. For each row, we use a unique fingerprint to instantiate a generator. And for each column, we feed in the same latent code to the generator instances. We validate the disentangled effect between latent code and fingerprint, which equips each generator instance with identical functionality.

Table 1. Fingerprint detection in bitwise accuracy and generation fidelity in FID.  $\uparrow/\downarrow$  indicates a higher/lower value is more desirable.

Method	CelebA			LSUN		
	Bit acc $\uparrow$	$p$ -value	FID $\downarrow$	Bit acc $\uparrow$	$p$ -value	FID $\downarrow$
StyleGAN2 [28]	-	-	9.37	-	-	19.24
[59]	0.989	$< 10^{-35}$	14.13	0.983	$< 10^{-34}$	21.31
Ours	0.991	$< 10^{-35}$	11.50	0.993	$< 10^{-35}$	20.50
Ours Variant I	0.999	$< 10^{-37}$	12.98	0.999	$< 10^{-37}$	20.68
Ours Variant II	0.987	$< 10^{-35}$	13.86	0.927	$< 10^{-25}$	21.70
Ours Variant III	0.990	$< 10^{-35}$	22.59	0.896	$< 10^{-21}$	64.91

performance, our method is substantially more efficient and scalable than theirs in practice, because they have to restart training with a new data collection for each fingerprint input. Preferably we can ad-hoc instantiate a large population of fingerprinted generators with little overhead.

We also compare to three architectural variants of our mechanism. The motivation of these variants is to preserve the original StyleGAN2 architecture as much as possible, especially for the latent code modulation. Variant I: We consider modulating convolutional filters with only the latent code embedding, while feeding the fingerprint code through the input of the generator. Variant II: We consider modulating filters twice, with the latent code embedding and our fingerprint code embedding separately. Variant III: We consider modulating filters with the embedding from the concatenation of the latent code and our fingerprint code.

**Results.** From Table 1, we find:

(1) On CelebA, all the methods achieve almost perfect fingerprint detection accuracy with sufficient confidence (small enough  $p$ -value). On LSUN, Ours Variant II and III do not achieve saturated performance. We reason that in our case filter modulation is dominated by fingerprint code already: fingerprint reconstruction loss has a stronger gradient than that of the adversarial loss. Modulating latent code can only increase the crosstalk between the two inputs.

(2) For the other methods achieving perfect detection accuracy on both datasets, Our method and Variant I have obvious advantages over [59] in practice: We can encode fingerprints with little overhead while they have to re-train for each fingerprint.

(3) Our method results in the optimal fidelity with slightly  $\leq 2.13$  FID degrading. It is the cost to multi-task with fingerprint detection, but is negligible and worthy. Therefore, our method is a desirable trade-off to achieves effectiveness and fidelity at the same time.

(4) Ours Variant I performs equally well to ours. However, it encodes fingerprints through the input of the generator, and thus is unable to instantiate different generator parameters for different deployments. Therefore, we stick to ours in the following experiments.

(5) We show in Figure 3 uncured generated samples from a variety of our generator instances. Image qualities are high. Fingerprints are imperceptible. And thanks to the consistency loss  $\mathcal{L}_{const}$ , different generator instances can generate identical images given the same latent code, while their fingerprints are still distinguishable by our decoder.

### 4.3. Capacity

The capacity indicates the number of unique fingerprints our mechanism can accommodate without crosstalk between two fingerprints. This is determined by the number of bits for fingerprint representation and by our detection accuracy (according to Section 4.2).

The choice of the number of bits is however non-trivial. A larger number can accommodate more unique fingerprints, but can also deteriorate fingerprint detection accuracy. This is because the limited number of fingerprint samples during training is not sufficient to cover the whole space, and as a result, cannot generalize in testing. A testing fingerprint is very likely not seen or cannot be well represented by training samples.

To figure out the optimal fingerprint bit length, we conduct the following experiments. On one hand, given one length, we evaluate our detection accuracy. On the other hand, we estimate the bottom line requirement for detection accuracy. This is calculated as the maximal bit overlap percentage among a large bag (1 million) of fingerprint samples. An ideal fingerprint detector should reach an accuracy that is not coarser than this overlap percentage.

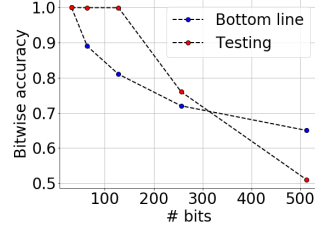


Figure 4. Fingerprint detection bitwise accuracy and its bottom line requirement w.r.t. fingerprint bit length on CelebA. The gap is maximized at bit length 128, which therefore becomes our choice.

In Figure 4, we vary the fingerprint bit length in the options of  $\{32, 64, 128, 256, 512\}$ , and plot the bitwise detection accuracy in red and the bottom line requirement in blue. We find:

(1) The bottom line requirement to detection accuracy is monotonically decreasing w.r.t. the bit length of fingerprint because, given a finite bag of fingerprint samples, the larger the bit length, the less likely two fingerprints overlap heavily.

(2) The testing accuracy is also monotonically decreasing w.r.t. the bit length of fingerprint. This is due to the generalization issue of fingerprint sampling, as aforementioned.

(3) The testing accuracy is empirically decreasing more slowly at the beginning and then faster than its bottom line requirement w.r.t. bit length. We therefore pick the bit length 128 as the optimal choice for which the gap between the two plots is maximized. We stick to this for all our experiments.

(4) Considering together our detection bitwise accuracy  $\geq 0.991$  and our fingerprint bit length 128, we derive in principle our mechanism can hold  $2^{128 \times 0.991} \approx 10^{36}$  distinct fingerprints and therefore can result in such a large capacity of identifiable generators.

### 4.4. Scalability

Scalability is one of the advantageous properties of our mechanism: During training we can efficiently instantiate a large capacity of generators with arbitrary fingerprints on the fly, so that fingerprint detection generalizes well for during testing. To validate this, we compare to baselines where we intentionally downgrade our method with access to only a fixed set of fingerprints. Without losing representativeness, these baselines stand for the category of non-scalable fingerprinting methods that have to re-train a generator instance for each fingerprint, e.g. [59]. We cannot directly compare to [59] because it is impractical (time-consuming) to instantiate a large number of their generators for analysis.

From Table 2 we show that fingerprint detection fails to generalize unless we can instantiate generators with 10k or more fingerprint samples. This indicates the necessity to

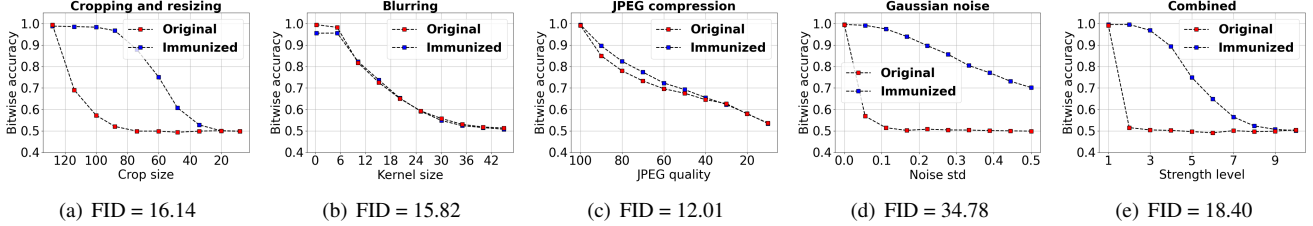


Figure 5. Red plots show, on CelebA, the fingerprint detection of our original model in bitwise accuracy w.r.t. the strength of perturbations. Blue plots show those of our immunized models. We consider accepting accuracy  $\geq 75\%$ . Therefore, our model is robust against blurring and JPEG compression, and is immunizable against cropping, Gaussian noise, and the combined perturbation. FID under each plot indicates the fidelity of each immunized model.

Table 2. Fingerprint detection in bitwise accuracy on CelebA during training and testing.  $\uparrow$  indicates a higher value is more desirable. Detection starts to generalize with 10k fingerprint training samples.

Fingerprint set size	Training accuracy $\uparrow$	Testing accuracy $\uparrow$
10	1.000	0.512
100	1.000	0.537
1k	1.000	0.752
10k	0.990	0.988
100k	0.983	0.981
Sampling on the fly	0.991	0.991

equip GANs with an efficient and scalable fingerprinting mechanism, preferably the one on the fly. The results show that we can stick to the principle to reach a capacity of  $10^{36}$ .

#### 4.5. Robustness and immunizability

Robustness against image perturbations is another advantageous property of our mechanism. When it does not hold for some perturbations, the immunizability property compensates for it.

The motivation to validate the robustness and immunizability of fingerprint detection lies in the fact that deep fakes in the open end may undergo post-processing environments and result in quality deterioration. We hereby evaluate the robustness against five types of image perturbation: cropping and resizing, blurring with Gaussian kernel, JPEG compression, additive Gaussian noise, and random combination of them. We consider two versions of our model: the original version and the immunized version. An immunized model indicates that during training we augment generated images with the corresponding perturbation in random strengths before feeding them to the fingerprint decoder.

We plot in Figure 5 the fingerprint detection accuracy of our original and immunized models w.r.t. the strength of each perturbation. We find:

(1) For all the perturbations, fingerprint detection accuracy drops monotonically as we increase the strength of perturbation. For some perturbations in red plots, i.e., blurring and JPEG compression, accuracy drops slowly in a reasonably large range. We consider accepting accuracy  $\geq 75\%$ . As a result, the robust working range under blurring is: Gaussian blur kernel size  $\sim [0, 7]$ ; under JPEG compression is: JPEG quality  $\sim [80, 100]$ . Usually the images turn not functional with perturbations heavier than this range. We therefore validate the robustness of our original model against blurring and JPEG compression.

(2) For the other perturbations, although our original model is not robust enough, immunization (perturbed augmentation) compensates significantly in blue dots. We consider accepting accuracy  $\geq 75\%$ . As a result, the immunized working range under cropping is: cropping size  $\sim [60, 128]$ ; under Gaussian noise is: noise standard deviation  $\sim [0.0, 0.4]$ ; under combined perturbation is: the combination of the robust or immunized working ranges aforementioned. Usually the images turn not functional with perturbations heavier than this range. We therefore validate the immunizability of our model against cropping, Gaussian noise, and the combined perturbation.

(3) We also report the FID of each immunized model in the sub-captions. Augmentation with perturbations indeed has a side effect on the adversarial training and consequently on fidelity. However, except for Gaussian noise immunization, the degrading from the others is to a reasonably small extent. We reason the challenge roots in the instability of adversarial training: the minimax formulation and alternating gradient ascent-descent.

#### 4.6. Deep fake detection and attribution

We have justified the effectiveness of our method for fingerprint detection. It in turn benefits our initial motivation: deep fake detection and attribution. The former task is a binary classification problem to distinguish between real and fake. The latter task is to further finely label the source of a generated image. We merge the two tasks into one with  $1+N$  classes: 1 real-world source and  $N$  GAN sources,

Table 3. Deep fake detection and attribution accuracy on CelebA. A higher value is more desirable. It is impractical to train too many classifiers when the number of GANs is large (e.g. 100) in the open world.

Scenario	#GANs	Classifier [57]	Ours
Closed world	1	0.997	1.000
	10	0.998	1.000
	100	0.955	1.000
Open world	1	0.893	1.000
	10	0.102	1.000
	100	N/A	1.000

where  $N$  can be extremely large, as large as our capacity  $10^{36}$  in Section 4.3.

Unlike previous methods that have to rely on inherent differences between real and fake [57, 52, 62, 12], our method *actively* encodes identifiable fingerprints into generator instances and consequently into the generated images. Then the tasks are converted to verifying if one decoded fingerprint is in our database or not. This is achieved by comparing the decoded fingerprint to each fingerprint in the database given a threshold of bit overlap. According to our  $\geq 0.991$  fingerprint detection accuracy and high confidence ( $p$ -value  $< 10^{-35}$ ). It should be reliable to set the threshold at  $128 \times 0.95 \approx 121$ . If the bit overlap is larger than this threshold, the fingerprint is verified in the database. Then the attribution is trivial because we can directly look up the generator instance according to the fingerprint. If the fingerprint is not in the database, it should be a random fingerprint decoded from a real image.

**Baseline.** Without losing representativeness, we compare to a recent deep fake detector/attribution [57] as a learning-based baseline relying on inherent visual clues. Because a learning-based method can only enumerate a small fixed set of training labels, we consider two scenarios for it: closed world and open world. The difference is whether the testing GAN sources are seen during training or not. This does not matter to our method because ours can work with any  $N \leq 10^{36}$ . For the closed world, we train/evaluate a baseline classifier on 10k/1k images from each of the  $N + 1$  sources. For the open world, we train  $N + 1$  1-vs-the-other binary classifiers, and predict as "the other" label if and only if all the classifiers predict negative results. We test on 1k images from each of the real source or  $N$  unseen GAN sources.

**Results.** From Table 3 we find:

(1) Deep fake detection and attribution based on our fingerprints perform equally perfectly ( $\sim 100\%$  accuracy) to that based on the classifier in the closed world, regardless of the number of seen GAN sources.

(2) Open world is also a trivial scenario to our method

Table 4. Fingerprint detection in bitwise accuracy and generation fidelity in FID w.r.t. the layer to modulate fingerprints.  $\uparrow/\downarrow$  indicates a higher/lower value is more desirable.

Layer	CelebA		LSUN	
	Bit acc $\uparrow$	FID $\downarrow$	Bit acc $\uparrow$	FID $\downarrow$
4×4	0.953	12.06	0.693	21.44
8×8	0.981	12.06	0.950	21.15
16×16	0.993	11.90	0.935	20.98
32×32	0.991	11.07	0.894	20.24
64×64	0.972	10.77	0.816	19.85
128×128	0.946	10.67	0.805	19.67
Ours (all layers)	0.991	11.50	0.993	20.50

but it challenges the baseline classifier. When the number of unseen GAN sources increases to 10, the classifier degenerates close to random guess. This is a common generalization issue of the learning-based method.

(3) It is even impractical to train too many (e.g. 100) 1-vs-the-other classifiers in the open world, due to its scalability limitation. Yet this is not an issue with our method.

(4) Since deep fake detection and attribution is a trivial task to our method, it makes our advantages independent of the evolution of GAN techniques, and orthogonal to how well a learning-based baseline performs. This suggests a novel direction for responsible disclosure.

#### 4.7. Ablation study on modulation

For completeness, as an ablation study we investigate the effectiveness of fingerprint detection and fidelity of generation when modulating fingerprint embeddings to different generator layers (resolutions).

From Table 4 we find:

(1) For effectiveness, the optimal single layer to modulate fingerprints appears in one of the middle layers, specific to datasets: 16×16 for CelebA and 8×8 for LSUN. But our all-layer modulation can achieve comparable or better performance. This should be consistent with different datasets because fingerprint detection turns more effective when we encode fingerprint to more parts of the generator.

(2) For fidelity, the side effect of fingerprinting is less significant if modulation happens in the shallower layer. This is because fingerprinting and generation are distinct tasks, and a shallower modulation leads to less crosstalk. However, considering the FID variance is not significant in general, we regard all-layer modulation as a desirable trade-off between effectiveness and fidelity.

## 5. Conclusion

One sustainable solution to mitigate the misuse of deep fakes is to enable a responsible disclosure of generative



models. We achieve this by a novel fingerprinting mechanism which allows researchers and companies to modulate their models with fingerprints, so that the generated samples containing a fingerprint can be accurately detected and attributed to a source. We formulate this as an efficient and scalable ad-hoc generation of a large population of models with distinct fingerprints. Experimental results show that our method fulfills several key properties: effectiveness, fidelity, large capacity, scalability, robustness, and immunizability. We validate its saturated performance and advantages over previous learning-based discriminative methods in the deep fake detection and attribution tasks, which makes it independent of the evolution of GAN techniques and agnostic to the other detection baselines.

## Acknowledgement

Ning Yu is partially supported by Twitch Fellowship. Vladislav Skripniuk is partially supported by IMPRS scholarship from Max Planck Institute. This work is also supported, in part, by the US Defense Advanced Research Projects Agency (DARPA) Media Forensics (MediFor) Program under FA87501620191 and Semantic Forensics (SemaFor) Program under HR001120C0124. Any opinions, findings, conclusions, or recommendations expressed in this material are those of the authors and do not necessarily reflect the views of the DARPA. We acknowledge the Maryland Advanced Research Computing Center for providing computing resources. We thank David Jacobs, Abhinav Shrivastava, and Yaser Yacoob for constructive advice in general.

## References

- [1] Rameen Abdal, Peihao Zhu, Niloy Mitra, and Peter Wonka. Styleflow: Attribute-conditioned exploration of stylegan-generated images using conditional continuous normalizing flows. *arXiv*, 2020. 1, 2
- [2] Darius Afchar, Vincent Nozick, Junichi Yamagishi, and Isao Echizen. Mesonet: a compact facial video forgery detection network. In *WIFS*, 2018. 3
- [3] Andrew Brock, Jeff Donahue, and Karen Simonyan. Large scale gan training for high fidelity natural image synthesis. In *ICLR*, 2018. 1, 2
- [4] Tom B Brown, Benjamin Mann, Nick Ryder, Melanie Subbiah, Jared Kaplan, Prafulla Dhariwal, Arvind Neelakantan, Pranav Shyam, Girish Sastry, Amanda Askell, et al. Language models are few-shot learners. *arXiv*, 2020. 1
- [5] Miles Brundage, Shahar Avin, Jack Clark, Helen Toner, Peter Eckersley, Ben Garfinkel, Allan Dafoe, Paul Scharre, Thomas Zeitzoff, Bobby Filar, et al. The malicious use of artificial intelligence: Forecasting, prevention, and mitigation. *arXiv*, 2018. 1, 2, 3
- [6] Long Chen, Hanwang Zhang, Jun Xiao, Liqiang Nie, Jian Shao, Wei Liu, and Tat-Seng Chua. Sca-cnn: Spatial and channel-wise attention in convolutional networks for image captioning. In *CVPR*, 2017. 3
- [7] Qifeng Chen and Vladlen Koltun. Photographic image synthesis with cascaded refinement networks. In *ICCV*, 2017. 1
- [8] Robert Chesney and Danielle Citron. Deepfakes and the new disinformation war: The coming age of post-truth geopolitics. *Foreign Aff.*, 2019. 1, 2, 3
- [9] Yunjey Choi, Minje Choi, Munyoung Kim, Jung-Woo Ha, Sunghun Kim, and Jaegul Choo. Stargan: Unified generative adversarial networks for multi-domain image-to-image translation. In *CVPR*, 2018. 1, 2
- [10] Yunjey Choi, Youngjung Uh, Jaejun Yoo, and Jung-Woo Ha. Stargan v2: Diverse image synthesis for multiple domains. In *CVPR*, 2020. 1, 2
- [11] Aysegul Dundar, Karan Sapra, Guilin Liu, Andrew Tao, and Bryan Catanzaro. Panoptic-based image synthesis. In *CVPR*, 2020. 2
- [12] Ricard Durall, Margret Keuper, and Janis Keuper. Watch your up-convolution: Cnn based generative deep neural networks are failing to reproduce spectral distributions. In *CVPR*, 2020. 1, 3, 8
- [13] Ricard Durall, Margret Keuper, Franz-Josef Pfrendt, and Janis Keuper. Unmasking deepfakes with simple features. *arXiv*, 2019. 1, 3
- [14] Joel Frank, Thorsten Eisenhofer, Lea Schönherr, Asja Fischer, Dorothea Kolossa, and Thorsten Holz. Leveraging frequency analysis for deep fake image recognition. In *ICML*, 2020. 1
- [15] Jun Fu, Jing Liu, Haijie Tian, Yong Li, Yongjun Bao, Zhiwei Fang, and Hanqing Lu. Dual attention network for scene segmentation. In *CVPR*, 2019. 3
- [16] Ian Goodfellow, Jean Pouget-Abadie, Mehdi Mirza, Bing Xu, David Warde-Farley, Sherjil Ozair, Aaron Courville, and Yoshua Bengio. Generative adversarial nets. In *NeurIPS*, 2014. 1, 2, 3
- [17] David Güera and Edward J Delp. Deepfake video detection using recurrent neural networks. In *AVSS*, 2018. 3
- [18] Ishaan Gulrajani, Faruk Ahmed, Martin Arjovsky, Vincent Dumoulin, and Aaron C Courville. Improved training of wasserstein gans. In *NeurIPS*, 2017. 1, 2
- [19] Douglas Harris. Deepfakes: False pornography is here and the law cannot protect you. *Duke L. & Tech. Rev.*, 2018. 1, 2, 3
- [20] Martin Heusel, Hubert Ramsauer, Thomas Unterthiner, Bernhard Nessler, and Sepp Hochreiter. Gans trained by a two time-scale update rule converge to a local nash equilibrium. In *NeurIPS*, 2017. 5
- [21] Chih-Chung Hsu, Chia-Yen Lee, and Yi-Xiu Zhuang. Learning to detect fake face images in the wild. In *IS3C*, 2018. 3
- [22] Xun Huang and Serge Belongie. Arbitrary style transfer in real-time with adaptive instance normalization. In *ICCV*, 2017. 3
- [23] Xun Huang, Ming-Yu Liu, Serge Belongie, and Jan Kautz. Multimodal unsupervised image-to-image translation. In *ECCV*, 2018. 2, 3

- [24] Phillip Isola, Jun-Yan Zhu, Tinghui Zhou, and Alexei A Efros. Image-to-image translation with conditional adversarial networks. In *CVPR*, 2017. 1, 2
- [25] Xu Jia, Bert De Brabandere, Tinne Tuytelaars, and Luc V Gool. Dynamic filter networks. In *NeurIPS*, 2016. 2, 3
- [26] Tero Karras, Timo Aila, Samuli Laine, and Jaakko Lehtinen. Progressive growing of gans for improved quality, stability, and variation. In *ICLR*, 2018. 1, 2
- [27] Tero Karras, Samuli Laine, and Timo Aila. A style-based generator architecture for generative adversarial networks. In *CVPR*, 2019. 1, 2, 3
- [28] Tero Karras, Samuli Laine, Miika Aittala, Janne Hellsten, Jaakko Lehtinen, and Timo Aila. Analyzing and improving the image quality of stylegan. In *CVPR*, 2020. 1, 2, 3, 4, 5, 12
- [29] Diederik P Kingma and Jimmy Ba. Adam: A method for stochastic optimization. 2015. 12
- [30] Diederik P Kingma and Max Welling. Auto-encoding variational bayes. In *ICLR*, 2014. 1
- [31] Orest Kupyn, Volodymyr Budzan, Mykola Mykhailych, Dmytro Mishkin, and Jiří Matas. Deblurgan: Blind motion deblurring using conditional adversarial networks. In *CVPR*, 2018. 1, 2
- [32] Orest Kupyn, Tetiana Martyniuk, Junru Wu, and Zhangyang Wang. Deblurgan-v2: Deblurring (orders-of-magnitude) faster and better. In *ICCV*, 2019. 1, 2
- [33] Anders Boesen Lindbo Larsen, Søren Kaae Sønderby, Hugo Larochelle, and Ole Winther. Autoencoding beyond pixels using a learned similarity metric. 2016. 1
- [34] Christian Ledig, Lucas Theis, Ferenc Huszár, Jose Caballero, Andrew Cunningham, Alejandro Acosta, Andrew Aitken, Alykhan Tejani, Johannes Totz, Zehan Wang, et al. Photo-realistic single image super-resolution using a generative adversarial network. In *CVPR*, 2017. 1, 2
- [35] Ke Li and Jitendra Malik. Implicit maximum likelihood estimation. *arXiv*, 2018. 1, 3
- [36] Ming-Yu Liu, Thomas Breuel, and Jan Kautz. Unsupervised image-to-image translation networks. In *NeurIPS*, 2017. 2, 3
- [37] Xihui Liu, Guojun Yin, Jing Shao, Xiaogang Wang, et al. Learning to predict layout-to-image conditional convolutions for semantic image synthesis. In *NeurIPS*, 2019. 1, 3
- [38] Ziwei Liu, Ping Luo, Xiaogang Wang, and Xiaoou Tang. Deep learning face attributes in the wild. In *ICCV*, 2015. 5, 12
- [39] Zhengzhe Liu, Xiaojuan Qi, Jiaya Jia, and Philip Torr. Global texture enhancement for fake face detection in the wild. In *CoRR*, 2020. 3
- [40] Francesco Marra, Diego Gagnaniello, Luisa Verdoliva, and Giovanni Poggi. Do gans leave artificial fingerprints? In *MIPR*, 2019. 1, 3
- [41] Takeru Miyato, Toshiki Kataoka, Masanori Koyama, and Yuichi Yoshida. Spectral normalization for generative adversarial networks. In *ICLR*, 2018. 1, 2
- [42] Xingang Pan, Xiaohang Zhan, Bo Dai, Dahua Lin, Chen Change Loy, and Ping Luo. Exploiting deep generative prior for versatile image restoration and manipulation. In *ECCV*, 2020. 1, 2
- [43] Taesung Park, Alexei A Efros, Richard Zhang, and Jun-Yan Zhu. Contrastive learning for unpaired image-to-image translation. In *ECCV*, 2020. 2
- [44] Taesung Park, Ming-Yu Liu, Ting-Chun Wang, and Jun-Yan Zhu. Semantic image synthesis with spatially-adaptive normalization. In *CVPR*, 2019. 1, 2, 3
- [45] Xiaojuan Qi, Qifeng Chen, Jiaya Jia, and Vladlen Koltun. Semi-parametric image synthesis. In *CVPR*, 2018. 1
- [46] Alec Radford, Luke Metz, and Soumith Chintala. Unsupervised representation learning with deep convolutional generative adversarial networks. In *ICLR*, 2016. 1, 2
- [47] Alec Radford, Jeffrey Wu, Rewon Child, David Luan, Dario Amodei, and Ilya Sutskever. Language models are unsupervised multitask learners. *OpenAI blog*, 2019. 1
- [48] Yujun Shen, Ceyuan Yang, Xiaoou Tang, and Bolei Zhou. Interfacegan: Interpreting the disentangled face representation learned by gans. In *CVPR*, 2020. 1, 2
- [49] Casper Kaae Sønderby, Jose Caballero, Lucas Theis, Wenzhe Shi, and Ferenc Huszár. Amortised map inference for image super-resolution. In *ICLR*, 2017. 1, 2
- [50] Akash Srivastava, Lazar Valkov, Chris Russell, Michael U Gutmann, and Charles Sutton. Veegan: Reducing mode collapse in gans using implicit variational learning. In *NeurIPS*, 2017. 3
- [51] Dmitry Ulyanov, Andrea Vedaldi, and Victor Lempitsky. Deep image prior. In *CVPR*, 2018. 1, 2
- [52] Sheng-Yu Wang, Oliver Wang, Richard Zhang, Andrew Owens, and Alexei A Efros. Cnn-generated images are surprisingly easy to spot... for now. In *CVPR*, 2020. 1, 3, 8
- [53] Ting-Chun Wang, Ming-Yu Liu, Jun-Yan Zhu, Andrew Tao, Jan Kautz, and Bryan Catanzaro. High-resolution image synthesis and semantic manipulation with conditional gans. In *CVPR*, 2018. 1, 2
- [54] Sanghyun Woo, Jongchan Park, Joon-Young Lee, and In So Kweon. Cbam: Convolutional block attention module. In *ECCV*, 2018. 3
- [55] Fuzhi Yang, Huan Yang, Jianlong Fu, Hongtao Lu, and Bain-ing Guo. Learning texture transformer network for image super-resolution. In *CVPR*, 2020. 3
- [56] Fisher Yu, Ari Seff, Yinda Zhang, Shuran Song, Thomas Funkhouser, and Jianxiong Xiao. Lsun: Construction of a large-scale image dataset using deep learning with humans in the loop. *arXiv*, 2015. 5, 12
- [57] Ning Yu, Larry S Davis, and Mario Fritz. Attributing fake images to gans: Learning and analyzing gan fingerprints. In *ICCV*, 2019. 1, 2, 3, 8
- [58] Ning Yu, Ke Li, Peng Zhou, Jitendra Malik, Larry Davis, and Mario Fritz. Inclusive gan: Improving data and minority coverage in generative models. In *ECCV*, 2020. 3
- [59] Ning Yu, Vladislav Skripniuk, Sahar Abdelnabi, and Mario Fritz. Artificial gan fingerprints: Rooting deepfake attribution in training data. *arXiv*, 2020. 3, 5, 6
- [60] Baiwu Zhang, Jin Peng Zhou, Iliia Shumailov, and Nicolas Papernot. Not my deepfake: Towards plausible deniability for machine-generated media. *arXiv*, 2020. 1
- [61] Richard Zhang, Phillip Isola, and Alexei A Efros. Colorful image colorization. In *ECCV*, 2016. 1, 2

- [62] Xu Zhang, Svebor Karaman, and Shih-Fu Chang. Detecting and simulating artifacts in gan fake images. In *WIFS*, 2019. 1, 3, 8
- [63] Hengshuang Zhao, Jiaya Jia, and Vladlen Koltun. Exploring self-attention for image recognition. In *CVPR*, 2020. 3
- [64] Jun-Yan Zhu, Taesung Park, Phillip Isola, and Alexei A Efros. Unpaired image-to-image translation using cycle-consistent adversarial networks. In *ICCV*, 2017. 2
- [65] Jun-Yan Zhu, Richard Zhang, Deepak Pathak, Trevor Darrell, Alexei A Efros, Oliver Wang, and Eli Shechtman. Toward multimodal image-to-image translation. In *NeurIPS*, 2017. 2

## 6. Supplementary material

### A. Implementation details

Our code is modified from the GitHub repository of StyleGAN2 [28] official TensorFlow implementation (config E)<sup>2</sup>. All the environment requirements, dependencies, data preparation, and command-line calling conventions are exactly inherited.

Our encoder  $E$  is composed of 8 fully-connected neural layers followed by LeakyReLU nonlinearity, the same as the  $\mathcal{Z} \mapsto \mathcal{W}$  mapping network in StyleGAN2 [28]. The generator  $G$  is almost the same as that in StyleGAN2 except we input the latent code  $z$  through the input end (replacing the learnable constant tensor) rather than through the modulation. The discriminator  $D$  is the same as that in StyleGAN2. The decoder  $F$  is almost the same as the discriminator except the output size is adapted to the latent code size plus the fingerprint size  $d_z + d_c$ .

We train our model using Adam optimizer [29] for 400 epochs. We use no exponential decay rate ( $\beta_1 = 0.0$ ) for the first moment estimates, and use the exponential decay rate  $\beta_2 = 0.99$  for the second moment estimates. The learning rate  $\eta = 0.002$ , the same as that in StyleGAN2. We train on 2 NVIDIA V100 GPUs with 16GB of memory each. Based on the memory available and the training performance, we set the batch size at 32. The training lasts for about 6 days.

### B. More generation results

Similar to Figure 3 in the main paper, we show in Figure 6 and 7 more uncured generated samples from a variety of generator instances trained on CelebA [38] or LSUN bedroom [56]. Image qualities are high. Fingerprints are imperceptible. Latent code and fingerprint are disentangled: generator instances with different fingerprints have an identical function.

---

<sup>2</sup><https://github.com/NVlabs/stylegan2>



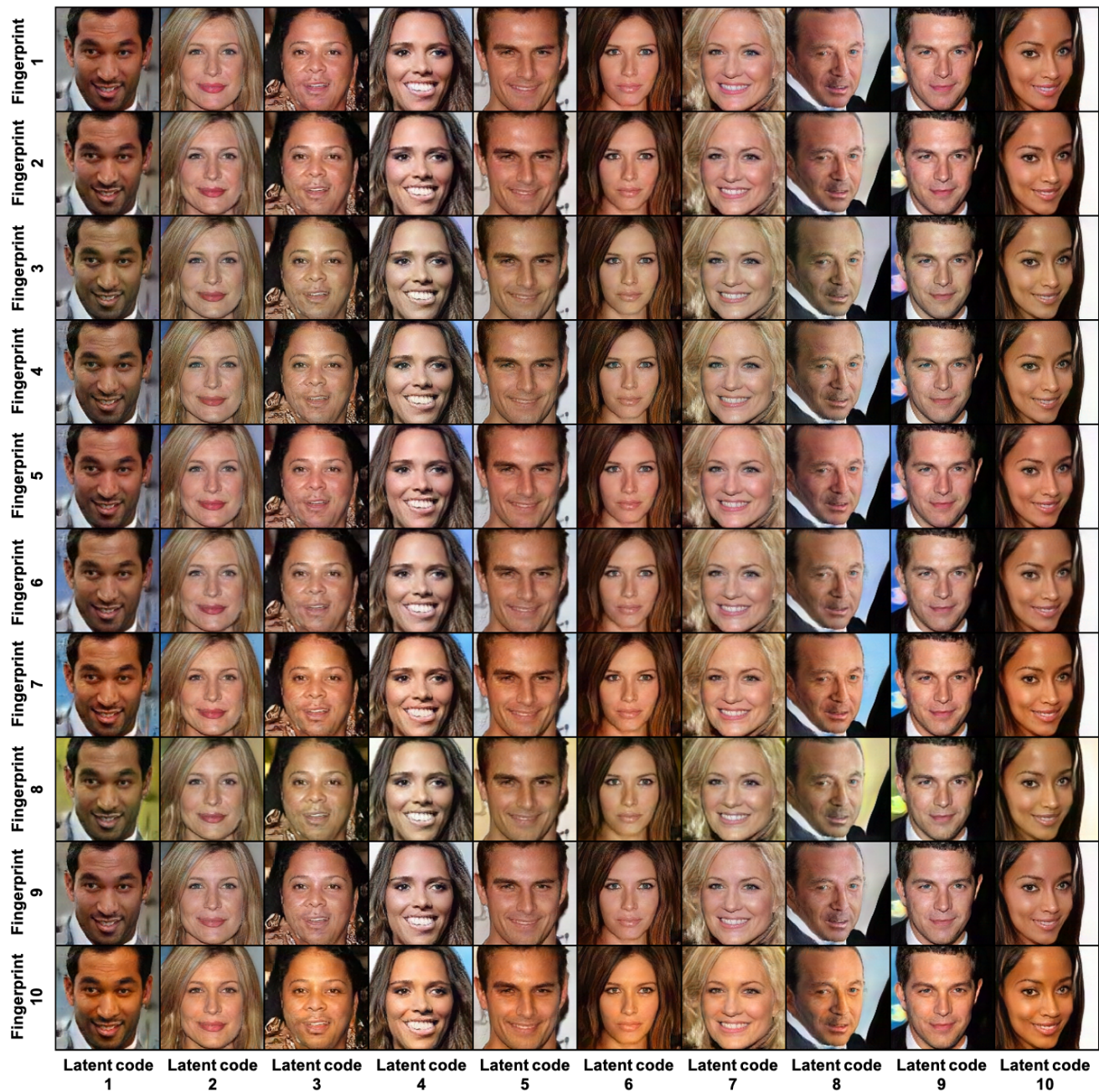


Figure 6. Generated samples from ten of our generator instances train on CelebA. For each row, we use a unique fingerprint to instantiate a generator. And for each column, we feed in the same latent code to the generator instances. We validate the disentangled effect between latent code and fingerprint, which equips each generator instance with identical functionality.



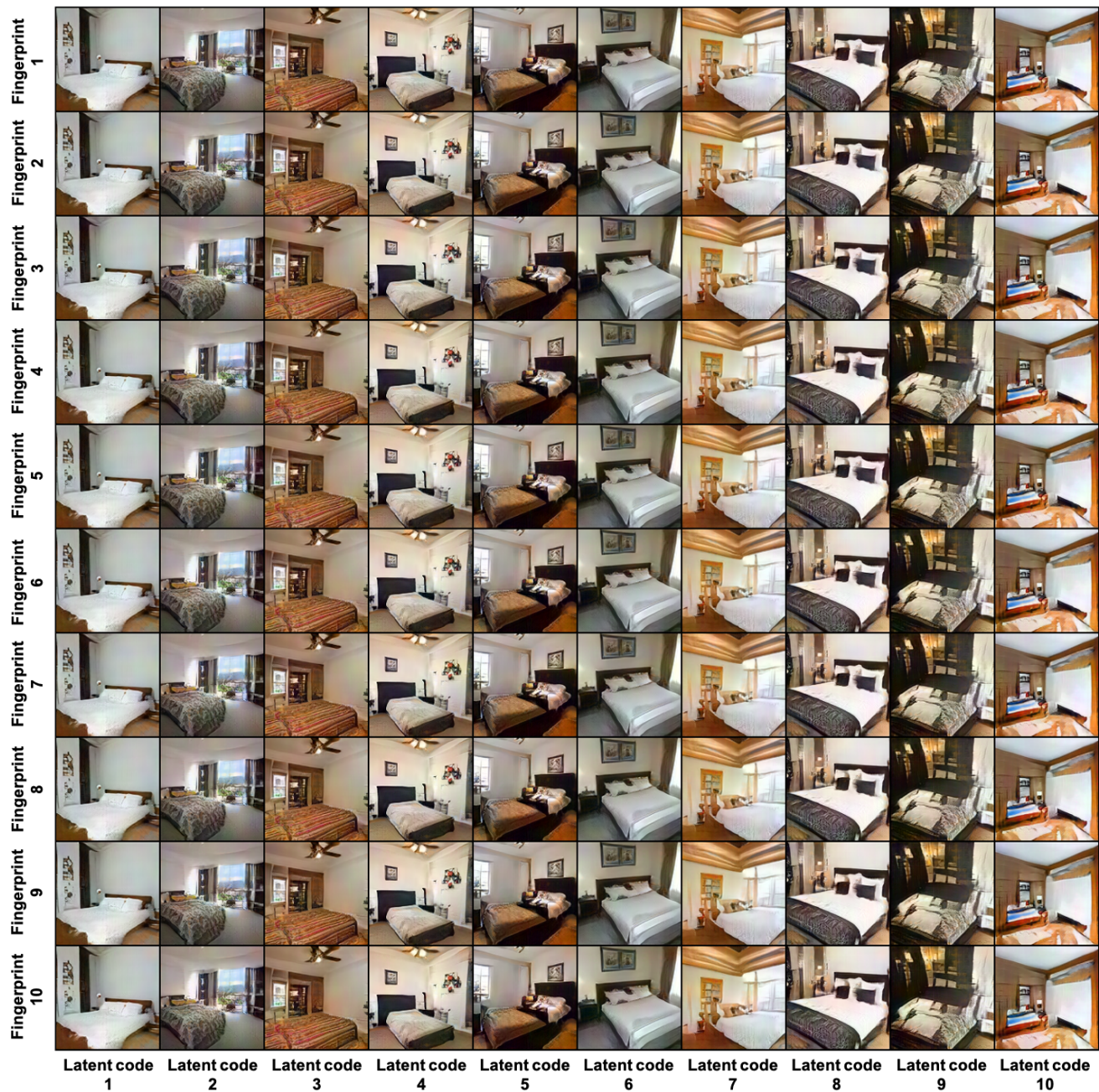


Figure 7. Generated samples from ten of our generator instances train on LSUN Bedroom. For each row, we use a unique fingerprint to instantiate a generator. And for each column, we feed in the same latent code to the generator instances. We validate the disentangled effect between latent code and fingerprint, which equips each generator instance with identical functionality.